Determination of the Magnetic Coupling in the Co/Cu/Co(100) System with Momentum-Resolved Quantum Well States

R. K. Kawakami,[1] E. Rotenberg,[2] Ernesto J. Escorcia-Aparicio,[1] Hyuk J. Choi,[1] J. H. Wolfe,[1] N. V. Smith,[2] and Z. Q. Qiu[1]

[1]*Department of Physics, University of California at Berkeley, Berkeley, California 94720*

[2]*Advanced Light Source, Lawrence Berkeley National Laboratory, Berkeley, California 94720*

(Received 26 October 1998)

The relation between the quantum well (QW) states and the oscillatory magnetic coupling in Co/Cu/Co grown on Cu(100) was investigated by angle resolved photoemission spectroscopy, magnetic x-ray linear dichroism, and the surface magneto-optic Kerr effect. The QW states were explained quantitatively using the phase accumulation model, and the derived QW phases at the Cu/Co interface were used to calculate the interlayer coupling. The agreement between this calculation and the experimental result reveals that the phase relation between the long- and short-period couplings is determined by the phase relation of the QW states in k space. [S0031-9007(99)09151-6]

PACS numbers: 75.70.Ak, 75.30.Kz, 75.30.Pd, 75.50.Bb

Quantum well (QW) states in metallic thin films were first observed in the nonmagnetic Ag/Au(111) system [1]. Later, it was shown that QW states also exist in a metal overlayer grown on a *ferromagnetic* substrate [2,3]. These discoveries promoted intense research on the intrinsic relation between the QW states and the oscillatory interlayer coupling [4,5] in the giant magnetoresistance (GMR) [6] magnetic multilayers. The QW nature of the interlayer coupling was identified from both the magnetic measurements [7,8] and a photoemission experiment [9]. Despite the great progress in the coupling study, several important issues remain unclear. One of the basic open questions is the relation of the long-period ($\sim$10–18 Å) and short-period ($\sim$3–6 Å) oscillations. Magnetic measurements suggest that the long- and short-period couplings are correlated with a relative phase and amplitude. Recent experiments revealed that the relative amplitudes depend sensitively on the interfacial roughness [10]. However, the origin of the relative phase between the long- and short-period couplings remains unclear. To better understand the origin of the interlayer couplings with different oscillation periodicities, several groups recently performed angle resolved photoemission spectroscopy (ARPES) experiments to investigate the QW states in k space. Segovia *et al.* studied the Cu/Co(100) system [11] at the neck of the Cu dog bone shape of the Fermi surface (see Fig. 1 of Ref. [11]), and identified the existence of the QW states from the binding energy spectra. The short-period oscillations in the density of states (DOS) at the neck of the Fermi level (E_F) was only recently observed by Kläsges *et al.* [12]. Curti *et al.* performed inverse photoemission for 2, 3, and 4 monolayers (ML) of Cu on Co(100) near the neck of the Fermi surface and focused on the dispersion of the QW energy with the in-plane momentum [13], but did not explore the relation between the long- and short-period oscillations. Li *et al.* studied the QW states in the Cr/Fe(100) system and identified the origin of the long-period oscillations in k space, but the existence of the short-period DOS oscillations at E_F was inconclusive [14]. Therefore, it has become very important to identify the relation of different QW states in k space to explore the relative phase of the long- and short-period interlayer couplings. In this Letter, we report results on the momentum-resolved QW states using ARPES as well as on the interlayer coupling using the magnetic x-ray linear dichroism (MXLD) and surface magneto-optic Kerr effect (SMOKE) on the Cu/Co(100) system. We first investigated the QW states in k space by doing ARPES on a Cu wedge grown on Co(100). We then studied the interlayer coupling using the MXLD and SMOKE techniques. With a direct comparison to the QW results obtained from the ARPES, we show that the QW phases at the Cu/Co interface in k space determine the relation of the long- and short-period oscillations in the interlayer coupling.

The experiment was performed using photoemission at the Advanced Light Source (ALS) at the Lawrence Berkeley National Laboratory. The fine focus (50–100 μm spot size) and high intensity ($>10^{12}$ photons per sec at a resolving power of 10 000) of the photon beam at beam line 7.0.1.2 enabled photoemission experiments on wedged samples with monolayer thickness resolution. The Cu(100) substrate was electropolished and cleaned with cycles of 2 keV Ar ion sputtering and annealing at $\sim$500–600 °C. A 15 ML Co film was first grown on the Cu to serve as the ferromagnetic substrate. The Cu wedge was grown on top of the Co by moving the substrate behind a knife-edge shutter. All films were grown at room temperature. Photoemission measurements were performed using a hemispherical analyzer. The total resolution (electron + photon) was better than 60 meV. The total angular acceptance was about 1.5°.

The results of the photoemission measurement on Cu(wedge)/Co(100) under normal emission (belly of the

 0031-9007/99/82(20)/4098(4)$15.00

Fermi surface) was reported previously [9]. To study the QW states at the neck of the Fermi surface, we performed the ARPES measurements by rotating the sample around the [011] axis with the detector position fixed. The QW states appearing near 11° and 77 eV photon energy correspond to the neck of the Fermi surface in the second Brillouin zone [11]. The image in Fig. 1 shows the energy spectra along the Cu wedge at this sample geometry. A smooth background arising from the Co and Cu $3d$ photoelectrons was subtracted out. The oscillations in the image clearly show the formation of the QW states near the neck of the Fermi surface.

To understand the QW energy spectra quantitatively, we employ the quantization condition derived from the phase accumulation method (PAM) [15].

$$2k_{\perp}^{e} d_{\mathrm{Cu}} - \phi_C - \phi_B = 2\pi\nu, \qquad \nu = \text{integer}, \quad (1)$$

where d_{Cu} is the thickness of the Cu layer, $k_{\perp}$ is the momentum in the normal direction of the film, k_{BZ} is the Brillouin zone vector, $k_{\perp}^{e} = k_{\mathrm{BZ}} - k_{\perp}$, and ϕ_B and ϕ_C are the phase gains of the electron wave function upon reflection at the Cu/vacuum and the Cu/Co interfaces, respectively.

To obtain the phases ϕ_B and ϕ_C, the upper (E_U) and lower (E_L) energies of the Co *minority-spin* energy band gap at the neck of the Cu Fermi surface are needed. For the 11° off-normal photoemission at 77 eV, the in-plane momentum is $k_{\parallel} = 0.87$ Å^{-1}. The values of E_U and E_L are 0.8 eV and -0.5 eV, respectively [16]. The ϕ_B and ϕ_C can then be calculated from the following formula [15]:

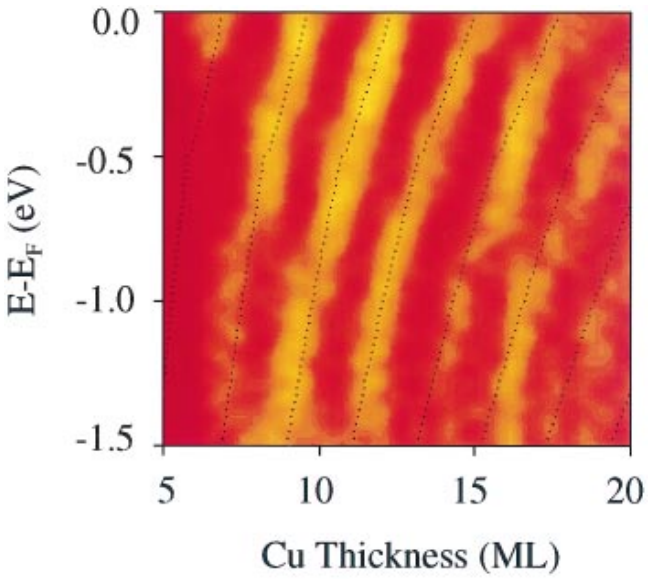

FIG. 1. Experimental results (color image) of the Cu QW states near the neck of the Fermi surface in the Cu/Co(100) system, and the theoretical calculation (dotted lines) using the phase accumulation model. ν is the QW index defined in Eq. (1). The DOS at E_{F} oscillates with ~2.7 ML periodicity.

$$\phi_B = \pi\sqrt{\frac{3.4\ (\mathrm{eV})}{4.4\ (\mathrm{eV}) - (E - \hbar^2 k_{\parallel}^2/2m)}} - \pi, \quad (2)$$

$$\phi_C = 2\sin^{-1}\sqrt{\frac{E - E_L}{E_U - E_L}} - \pi. \quad (3)$$

Here the energy E is measured from the Fermi level, 4.4 eV is the work function of Cu [17], and $k_{\parallel}$ is the in-plane component of the momentum which is conserved for ARPES. The perpendicular component of the Fermi wave vector ($k_{\mathrm{F}\perp}$) was taken as 1.1 Å^{-1} to account for the 2.7 ML oscillation periodicity at the Fermi level. Since the Cu band near the neck of the Fermi surface is very close to the free electron band [16], we adopted the dispersion of $E(k_{\perp}) = G(k_{\perp}^2/k_{\mathrm{F}\perp}^2 - 1)$ with G as the only fitting parameter. The dotted lines in Fig. 1 depict the fitting results using $G = 4.7$ eV. The agreement with the experimental data indicates that the QW states at the neck of the Fermi surface are accurately described by the PAM using the theoretical values of E_U and E_L.

It is important to point out that E_{F} at the neck of the Fermi surface is within the Co energy gap ($E_U > E_{\mathrm{F}} > E_L$), in contrast to the belly of the Fermi surface where E_{F} is above the Co energy gap ($E_{\mathrm{F}} > E_U > E_L$). This difference leads to the formation of the bound QW states at the neck of the Fermi surface as opposed to the resonant QW states at the belly of the Fermi surface [16,18]. In terms of the PAM, a negative phase ($\phi_C = -0.57\pi$) is derived at the neck of the Fermi surface as opposed to the zero phase ($\phi_C = 0$) at the belly of the Fermi surface. This is the origin of the phase relation between the long- and short-period couplings.

We utilized magnetic x-ray linear dichroism (MXLD) in the Co $3p$ normal photoemission to measure the Co magnetization [19]. The incident 130 eV photon beam was p polarized (in the plane of incidence) with an incident angle of $\theta = 30°$ (measured from sample surface). Figure 2 shows the $3p$ core-level spectra from a 15 ML Co film grown on Cu(100). The $+$M and $-$M are the two opposite magnetization directions which are in the film plane but perpendicular to the photon incident plane. The MXLD asymmetry, defined as $[\mathrm{I}(+\mathrm{M}) - \mathrm{I}(-\mathrm{M})]/[\mathrm{I}(+\mathrm{M}) + \mathrm{I}(-\mathrm{M})]$, measures the presence of magnetic ordering and is sensitive to the magnetization direction. To ensure a direct comparison of the QW states and the magnetic coupling, we covered half of the Cu(wedge)/Co(100) with a 3 ML Co film [Fig. 3(a)] so that the QW states and the magnetic interlayer coupling can be obtained from each half of the sample. Images of the DOS at the belly [Fig. 3(b)] and neck [Fig. 3(c)] of the Fermi surface were obtained by scanning the photon beam across the Cu wedge on the Cu/Co(100) side of the sample using the methods discussed earlier. The sample was then magnetized with a pulsed magnetic field to saturate the magnetization of the 15 ML Co. Because of the surface sensitivity, the MXLD measures the magnetization of the top 3 ML Co only. Therefore, the MXLD asymmetry

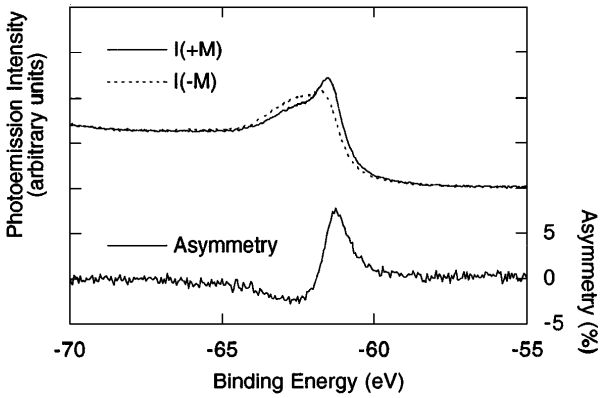

FIG. 2. MXLD spectra and the asymmetry from a 15 ML Co film.

measurements across the Co/Cu(wedge)/Co sandwich will identify the alternating magnetization direction of the 3 ML Co as a result of the oscillatory interlayer coupling. Figure 3(d) shows the image of the peak values of the MXLD asymmetry across the Co/Cu/Co(100) side of the sample, with the high- and low-intensity regions corresponding to the antiferromagnetic (AF) and ferromagnetic (FM) couplings, respectively.

It is well known that the oscillatory interlayer coupling in Fig. 3(d) consists of two periodicities which come from the spanning vectors at the belly and neck of the Fermi surface. The total coupling, therefore, is usually expressed by the formula

$$J = -\frac{A_1}{d_{\mathrm{Cu}}^2}\sin\left(\frac{2\pi d_{\mathrm{Cu}}}{\Lambda_1} + \Phi_1\right) - \frac{A_2}{d_{\mathrm{Cu}}^2}\sin\left(\frac{2\pi d_{\mathrm{Cu}}}{\Lambda_2} + \Phi_2\right). \quad (4)$$

Here d_{Cu} is the Cu thickness, $\Lambda_1 = \pi/k_{\perp 1}^e = 5.6$ ML and $\Lambda_2 = \pi/k_{\perp 2}^e = 2.7$ ML are the long and short periods, and positive J indicates the antiferromagnetic coupling. Experimental data are usually fitted with Eq. (4) to derive the amplitudes and the phases. It was shown that the relative amplitude A_2/A_1 depends on the surface roughness [10], but the relative phase is not well understood [20]. Since the magnetic coupling comes from the QW states, the values of Φ_1 and Φ_2 must be intrinsically related to the QW phases (ϕ_C) at the belly and neck of the Fermi surface. The QW coupling is determined by the energy difference of the spacer layer between parallel and antiparallel alignment of the two ferromagnetic layers, i.e., $2J \approx E_{\mathrm{P}} - E_{\mathrm{AP}} = \int_{-\infty}^{E_{\mathrm{F}}} E\Delta D\, dE$, where $\Delta D = D_{\mathrm{P}} - D_{\mathrm{AP}}$ is the difference of the density of states between the parallel and antiparallel alignment of the two ferromagnetic layers. As a QW state crosses the Fermi level, it adds energy to E_{P}, leading to the antiferromagnetic coupling. When the QW states are truly confined, ΔD is a set of delta functions so that the antiferromagnetic coupling peak corresponds exactly to the presence of a QW state at the Fermi level. For resonant states, however, the antiferromagnetic coupling peak no longer coincides exactly with the QW peak at the Fermi level due to the broadening of the QW state [21,22]. In the case of Co/Cu/Co(100), the first antiferromagnetic coupling peak of the long-period oscillations is at ~7 ML [16] which is about a 1 ML shift from the QW peak (~6 ML). Our previous results [9] shows that a bulk electron band of Cu works very well for QW states as the Cu thickness is greater than 4 ML. Thus, it is justified to determine the thickness shift from the result of Ref. [16]. At the neck of the Fermi surface, the minority spin electrons are completely confined ($E_U > E_{\mathrm{F}} > E_L, \Phi_C = -0.57\pi$) so that the quantization condition at E_{F} coincides with the maxima of J. Noting that the quantization condition for Co/Cu/Co should be $2k_{\perp}^e d_{\mathrm{Cu}} - 2\phi_C = 2\pi\nu$ instead of the $2k_{\perp}^e d_{\mathrm{Cu}} - \phi_C - \phi_B = 2\pi\nu$ for the Cu/Co case, it is easy to derive that $\Phi_2 = -\pi/2 - 2\phi_C = 0.64\pi$. At the belly of the Fermi

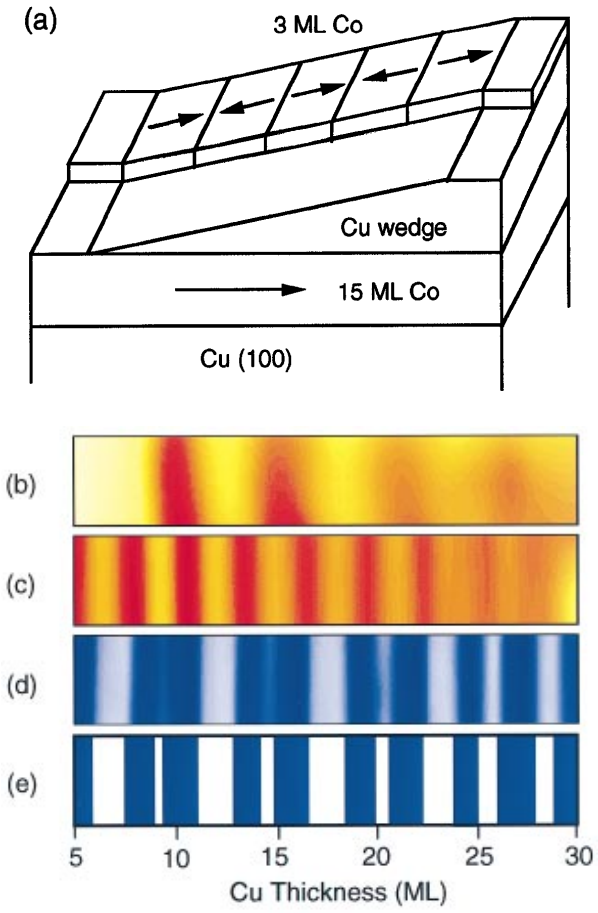

FIG. 3. (a) Schematic drawing of the sample from which both QW states and the interlayer coupling were obtained. (b) (color) DOS at the belly of the Fermi surface oscillates with 5.6 ML periodicity of the Cu thickness. (c) (color) DOS at the neck of the Fermi surface oscillates with 2.7 ML periodicity of the Cu thickness. (d) (color) Interlayer coupling from the MXLD measurements. The white and dark regions correspond to the antiferromagnetic and ferromagnetic interlayer couplings. (e) (color) Interlayer coupling calculated from Eq. (4) (see text). The white and dark regions correspond to the antiferromagnetic and ferromagnetic interlayer couplings.

surface, the minority electrons are only partially confined ($E_L < E_U < E_F$, $\Phi_C = 0$) so that the 1 ML shift between the QW peak and the antiferromagnetic coupling peak has to be taken into account. This will give a phase shift of $2\pi/\Lambda_1 = 0.36\pi$ between the interlayer coupling and the quantization condition at the belly of the Fermi surface, so that $\Phi_1 = -\pi/2 - 0.36\pi = -0.86\pi$. With the values of $\Phi_1 = -0.86\pi$ and $\Phi_2 = 0.64\pi$, we used the sign of Eq. (4) to fit the MXLD result with A_2/A_1 as the fitting parameter. The fitting result, with a value of $A_2/A_1 = 1.2 \pm 0.1$, is shown in Fig. 3(e) as the white (AF coupling) and blue (FM coupling) stripes. The AF and FM coupling positions from the fitting agree very well with the experimental data. Since the MXLD measurement gives only the sign of the coupling, we performed a surface magneto-optic Kerr effect (SMOKE) measurement to test the amplitude of Eq. (4). Hysteresis loops were taken for a Co(10 ML)/Cu(wedge)/Co(10 ML) sandwich, and the antiferromagnetic coupling strength was determined using the same method as in Ref. [23]. The result is shown in Fig. 4 together with the calculated antiferromagnetic coupling strength from Eq. (4) using the same A_2/A_1 ratio as in Fig. 3(e). The overall agreement between the SMOKE results and the calculated antiferromagnetic coupling strength is very good. The discrepancy in the width of the AF coupling peak is due to the finite size of the SMOKE laser beam. The above results show that the long- and short-period interlayer couplings are well determined by the QW states in k space.

In summary, the QW states near the belly and neck of the Fermi surface in the Cu/Co(100) system were studied by ARPES and were explained quantitatively by the PAM. The phase relation between the long- and short-period Fermi level QW states was used to determine the magnetic interlayer coupling. The calculated result was shown to agree very well with the MXLD and SMOKE measurements on the Co/Cu/Co(100) system.

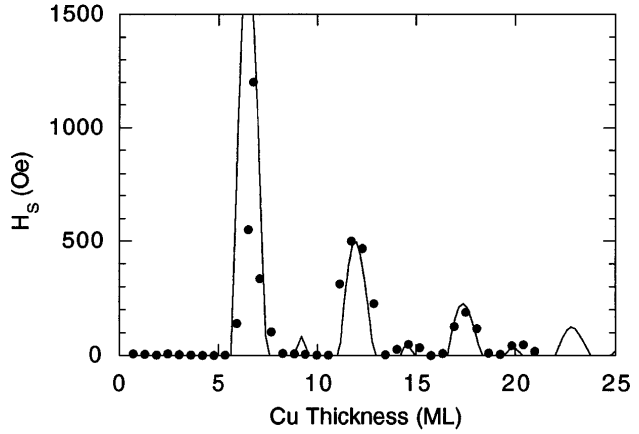

FIG. 4. SMOKE measurement across the Co(10 ML)/Cu(wedge)/Co(10 ML) sandwich (solid dots) with the calculated results (solid line) from Eq. (4) using the same A_2/A_1 ratio as in Fig. 3(e).

We acknowledge helpful discussions with Y. R. Shen. This work was funded by DOE Contract No. DE-AC03-76SF00098 and NSF DMR-9805222, and was also supported in part by the University of California for the conduct of discretionary research by Los Alamos National Laboratory.

[1] T. Miller, A. Samsavar, G. E. Franklin, and T.-C. Chiang, Phys. Rev. Lett. **61**, 1404 (1988).
[2] J. E. Ortega and F. J. Himpsel, Phys. Rev. Lett. **69**, 844 (1992).
[3] K. Garrison, Y. Chang, and P. D. Johnson, Phys. Rev. Lett. **71**, 2801 (1993).
[4] P. Grünberg, R. Schreiber, Y. Pang, M. B. Brodsky, and H. Sowers, Phys. Rev. Lett. **57**, 2442 (1986).
[5] S. S. P. Parkin, N. More, and K. P. Roche, Phys. Rev. Lett. **64**, 2304 (1990).
[6] M. N. Baibich, J. M. Broto, A. Fert, F. Nguyen Van Dau, F. Petroff, P. Etienne, G. Creuzet, A. Friedrich, and J. Chazelas, Phys. Rev. Lett. **61**, 2472 (1988).
[7] P. J. H. Bloemen, M. T. Johnson, M. T. H. van de Vorst, R. Coehoorn, J. J. de Vries, R. Jungblut, J. aan de Stegge, A. Reinders, and W. J. M. de Jonge, Phys. Rev. Lett. **72**, 764 (1994).
[8] S. N. Okuno and K. Inomata, Phys. Rev. Lett. **72**, 1553 (1994); Phys. Rev. B **51**, 6139 (1995).
[9] R. K. Kawakami, E. Rotenberg, Ernesto J. Escorcia-Aparicio, Hyuk J. Choi, T. R. Cummins, J. G. Tobin, N. V. Smith, and Z. Q. Qiu, Phys. Rev. Lett. **80**, 1754 (1998).
[10] J. Unguris, R. J. Celotta, and D. T. Pierce, Phys. Rev. Lett. **79**, 2734 (1997).
[11] P. Segovia, E. G. Michel, and J. E. Ortega, Phys. Rev. Lett. **77**, 3455 (1996).
[12] R. Kläsges, D. Schmitz, C. Carbone, W. Eberhardt, P. Lang, R. Zeller, and P. H. Dederichs, Phys. Rev. B **57**, R696 (1998).
[13] F. G. Curti, A. Danese, and R. A. Bartynski, Phys. Rev. Lett. **80**, 2213 (1998).
[14] Dongqi Li, J. Pearson, S. D. Bader, E. Vescovo, D.-J. Huang, P. D. Johnson, and B. Heinrich, Phys. Rev. Lett. **78**, 1154 (1997).
[15] N. V. Smith, N. B. Brookes, Y. Chang, and P. D. Johnson, Phys. Rev. B **49**, 332 (1994).
[16] J. Mathon, Murielle Villeret, R. B. Muniz, J. d'Albuquerque e Castro, and D. M. Edwards, Phys. Rev. Lett. **74**, 3696 (1995).
[17] V. S. Fomenko, *Handbook of Thermionic Properties*, edited by G. V. Samsanov (Plenum Press Data Division, New York, 1966).
[18] M. C. Munoz and J. L. Perez-Diaz, Phys. Rev. Lett. **72**, 2482 (1994).
[19] Ch. Roth, F. U. Hillebrecht, H. B. Rose, and E. Kisker, Phys. Rev. Lett. **70**, 3479 (1993).
[20] W. Weber, R. Allenspach, and A. Bischof, Europhys. Lett. **31**, 491 (1995).
[21] P. Bruno and C. Chappert, Phys. Rev. Lett. **67**, 1602 (1991).
[22] P. Bruno, Phys. Rev. B **52**, 411 (1995).
[23] Z. Q. Qiu, J. Pearson, and S. D. Bader, Phys. Rev. B **46**, 8659 (1992).